M. SZYMAŃSKI,[1] M. BLUHM,[1, 2, 3] K. REDLICH,[1, 3] C. SASAKI[1]

[1] Institute of Theoretical Physics, University of Wrocław
  (PL-50204 Wrocław, Poland; e-mail: michal.szymanski@ift.uni.wroc.pl)
[2] SUBATECH UMR 6457 (IMT Atlantique, Université de Nantes, IN2P3/CNRS)
  (4 rue Alfred Kastler, 44307 Nantes, France)
[3] Extreme Matter Institute EMMI, GSI
  (Planckstr. 1, D-64291 Darmstadt, Germany)

SEARCHING FOR THE QCD CRITICAL POINT WITH NET-PROTON NUMBER FLUCTUATIONS

Net-proton number fluctuations can be measured experimentally and, hence, provide a source of important information about the matter created during relativistic heavy ion collisions. Particularly, they may give us clues about the conjectured QCD critical point. In this work, the beam-energy dependence of ratios of the first four cumulants of the net-proton number is discussed. These quantities are calculated using a phenomenologically motivated model in which critical mode fluctuations couple to protons and antiprotons. Our model qualitatively captures both the monotonic behavior of the lowest-order ratio, as well as the non-monotonic behavior of higher-order ratios, as seen in the experimental data from the STAR Collaboration. We also discuss the dependence of our results on the coupling strength and the location of the critical point.

K e y w o r d s: net-proton number fluctuations, QCD critical point, heavy-ion collisions.

1. Introduction

The theoretical and experimental investigations of the phase diagram of strongly interacting matter are an important subject of modern high-energy physics. One of the unresolved questions concerns the existence and location of the QCD critical point (CP) in the T and μ planes. Strong fluctuations of the critical mode, σ, in the vicinity of CP, although not directly observable, are expected to couple to physically measurable quantities such as fluctuations of conserved charges [1, 2].

Fluctuations of the net-proton number serve as an experimental probe of baryon number fluctuations. Recent, but still preliminary results of the STAR Collaboration [3–5] show a non-monotonic beam energy dependence of the ratios of higher-order net-proton number cumulants. However, the interpretation of the data is still unclear [6–9]. Therefore, effective models are needed to improve our understanding of these quantities.

One of such models was developed in [10], where the impact of resonance decays on net-proton num-

ber cumulant ratios was studied. This model could qualitatively describe the non-monotonic behavior of the C_3/C_2 and C_4/C_2 ratios. However, it also showed a strong non-monotonic behavior of the C_2/C_1 ratio which is not observed experimentally. Recently, this model was re-examined [11] to account for the scaling properties of the baryon number and chiral susceptibilities obtained within effective models [12, 13]. This reduces the effect of critical fluctuations in the net-proton number variance and, thus, allows for a better description of the STAR data.

Here, we discuss the beam energy dependence of the ratios of net-proton number cumulants obtained using the refined model from Ref. [11] and study their dependence on the coupling strength between the critical mode and (anti)protons, as well as their dependence on the location of the critical point.

2. Model Setup

As a baseline model to calculate the net-proton number cumulants, we choose the hadron resonance gas (HRG) model in which the number density of each particle species is given by the ideal gas formula,

$$n_i(T, \mu_i) = d_i \int \frac{d^3k}{(2\pi)^3} f_i^0(T, \mu_i). \tag{1}$$

Here, d_i is the degeneracy factor, and

$$f_i^0 = \frac{1}{(-1)^{B_i} + e^{(E_i - \mu_i)/T}} \tag{2}$$

is the equilibrium distribution function, where $E_i = \sqrt{\mathbf{p}^2 + m_i^2}$ is the dispersion relation, and $\mu_i = B_i\mu_B + S_i\mu_S + Q_i\mu_Q$ is the chemical potential of a particle with mass m_i, baryon number B_i, strangeness S_i, and electric charge Q_i; μ_B, μ_Q and μ_S denote the baryon, strangeness and charge chemical potentials.

Since the QCD pressure is approximated in the HRG model by a sum of partial ideal gas pressures corresponding to different particles, there are only thermal fluctuations in this approximation. To include critical fluctuations on the top of thermal ones, we follow the phenomenological approach employed in Ref. [10]. In this approach, the particle mass is assumed to be composed of critical and non-critical parts as suggested in linear sigma models,

$$m_i \sim m_0 + g_i\sigma, \tag{3}$$

where m_0 is a non-critical contribution, and g_i is the coupling strength between the critical mode and the particle of type i. Critical mode fluctuations modify the distribution function into $f_i = f_i^0 + \delta f_i$, where a change of the distribution function due to critical mode fluctuations reads

$$\delta f_i = \frac{\partial f_i}{\partial m_i}\delta m_i = -\frac{g_i}{T}\frac{v_i^2}{\gamma_i}\delta\sigma, \tag{4}$$

with $v_i^2 = f_i^0((-1)^{B_i}f_i^0 + 1)$ and $\gamma_i = E_i/m_i$.

Fluctuations of the particle number in the thermal medium can be quantified in terms of cumulants. The n-th order cumulant of the i-th particle species reads

$$C_n^i = VT^3\frac{\partial^{n-1}(n_i/T^3)}{\partial(\mu_i/T)^{n-1}}\bigg|_T, \tag{5}$$

where the temperature T is kept constant. In this work, we consider the first four cumulants of the net-proton number, $N_{p-\bar{p}} = N_p - N_{\bar{p}}$, which are given by [10]

$$C_n = C_n^p + (-1)^n C_n^{\bar{p}} +$$
$$+ (-1)^n \langle(V\delta\sigma)^n\rangle_c (m_p)^n (J_p - J_{\bar{p}})^n, \tag{6}$$

where C_n^p and $C_n^{\bar{p}}$ are the n-th order proton and antiproton cumulants obtained within the baseline

model, respectively, $\langle(V\delta\sigma)^n\rangle_c$ is the n-th critical mode cumulant, and

$$J_i = \frac{gd}{T}\int\frac{d^3k}{(2\pi)^3}\frac{1}{E}f_i^0(1 - f_i^0). \tag{7}$$

Moreover, the contributions of other particles and resonance decays are neglected.

In general, cumulants of the critical mode cannot be calculated analytically. Following the approach introduced in Ref. [10], we model them using the universality class arguments which state that different physical systems belonging to the same universality class exhibit the same critical behavior close to the critical point [14]. Under the assumption that QCD belongs to the same universality class, as the three-dimensional Ising model [16–18], we can identify the QCD order parameter, σ, with the magnetization, M_I, the order parameter of the spin model. Hence, the critical mode cumulants can be written as [10]

$$\langle(V\delta\sigma)^n\rangle_c = \left(\frac{T}{VH_0}\right)^{n-1}\frac{\partial^{n-1}M_I}{\partial h^{n-1}}\bigg|_r, \tag{8}$$

where $r = (T - T_c)/T_c$ is the reduced temperature, and $h = H/H_0$ is the reduced magnetic field. The critical point is located at $r = h = 0$.

In the net-proton number cumulants, the singular part of the second cumulant receives a contribution from the first derivative of the order parameter with respect to the reduced magnetic field,

$$C_2^{\text{sing.}} \propto \frac{\partial M_I}{\partial h}. \tag{9}$$

The right-hand side of this equation is the magnetic susceptibility of the Ising model which, due to universality, can be identified with the chiral susceptibility of QCD. However, C_2 is related to the baryon number susceptibility which is known to diverge weaker than the chiral one [12, 13, 19]. Therefore, the model introduced in Ref. [10] requires some modifications [11]. This can be done using the following relation obtained by calculations within the effective model on the mean field level [12, 13]:

$$\chi_{\mu\mu} \simeq \chi_{\mu\mu}^{\text{reg}} + \sigma^2\chi_{\text{chiral}}, \tag{10}$$

in which the singular contribution to the baryon number susceptibility is proportional to the chiral susceptibility times the squared order parameter, and $\chi_{\mu\mu}^{\text{reg}}$
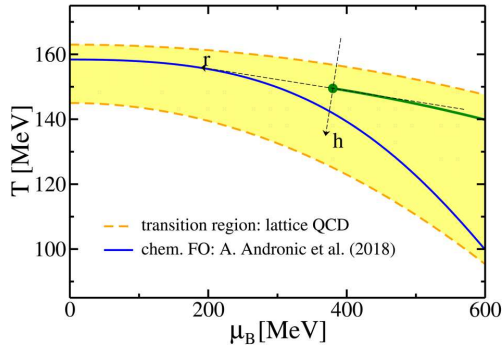
Fig. 1. (Color online) The model setup used in this work. The filled band between two dashed curves shows the lattice QCD constraints for the chiral crossover transition. The green dot denotes the critical point with the spin model coordinate system attached to it and the first-order phase transition line for a larger baryon chemical potential. The solid blue line corresponds to the chemical freeze-out curve from [15]

is the regular part of the baryon number susceptibility. To obtain such a form of the second cumulant, the proton mass in Eq. (6) should be replaced by the order parameter, σ, such that the new C_2 reads

$$C_2 = C_2^p + C_2^{\bar{p}} + g^2\sigma^2\langle (V\delta\sigma)^n\rangle (J_p - J_{\bar{p}})^2. \quad (11)$$

The modified higher-order cumulants are

$$C_3 = C_3^p - C_3^{\bar{p}} - g^3\sigma^3\langle (V\delta\sigma)^n\rangle (J_p - J_{\bar{p}})^3 \quad (12)$$

and

$$C_4 = C_4^p + C_4^{\bar{p}} + g^4\sigma^4\langle (V\delta\sigma)^n\rangle (J_p - J_{\bar{p}})^4. \quad (13)$$

Since the cumulants are volume-dependent, it is convenient to consider their ratios in which this dependence cancels out,

$$\frac{C_2}{C_1} = \frac{\sigma^2}{M}, \quad \frac{C_3}{C_2} = S\sigma, \quad \frac{C_4}{C_2} = \kappa\sigma^2, \quad (14)$$

where $M = C_1$ is the mean, $\sigma^2 = C_2$ the variance, $\kappa = C_4/C_2^2$ the kurtosis, and $S = C_3/C_2^{3/2}$ the skewness.

To use the universality class arguments discussed above, a mapping between the QCD phase diagram and the reduced temperature and a magnetic field of the spin model is needed. Such a mapping is non-universal and has to be modeled for each system separately. In this work, we use a linear mapping [20, 21] in which the critical point is located at $r = h = 0$, the r axis is tangential to the QCD first-order phase transition line, and the positive direction of the h axis points toward the hadronic phase. Schematically, this is shown in Fig. 1, where the green line denotes the first-order phase transition, and the filled band shows lattice QCD constraints on the location of the chiral crossover region.

To calculate the order parameter and its cumulants, we use the parametric representation of the magnetic equation of state [22]. For a more detailed discussion of the mapping, lattice limits, and the magnetic equation of state, we refer the reader to the papers [10, 11].

Finally, assuming that the matter created during a heavy ion collision forms a thermal medium characterized by the temperature and chemical potentials, experimental data on event-by-event multiplicity fluctuations can be compared with model results. To this end, we calculate the net-proton number cumulants at the chemical freeze-out. The chemical freeze-out conditions used in this work were obtained by the analysis of hadron yields [23–28]. The blue line in Fig. 1 shows the recently obtained parametrization [15].

3. Numerical Results

In this section, we discuss numerical results on net-proton number cumulant ratios obtained within the current model. The set of model parameters includes the coupling strength g between (anti)protons and the critical mode, the parameters of the magnetic equation of state, as well as the size of a critical region in the (T, μ) plane. Their values and a detailed discussion can be found in Refs. [10, 11]. Moreover, the location of the QCD critical point is unknown. To study the effect of its position in the QCD phase diagram on the refined model results, we consider three different locations of the CP listed in Table and shown in Fig. 2, where the distance to the freeze-out curve is the farthest for CP_1 and closest for CP_3.

The first step of our discussion is the comparison between the C_2/C_1 ratio obtained using the model from Ref. [10], where the n-th net-proton number cumulant is given by Eq. (6), and the refined model [11] for the critical point location CP_1. This is shown in Fig. 3. Results obtained using the original model exhibit a clear non-monotonic behavior and deviate strongly from the non-critical baseline (the black-dotted line) even for the small coupling, $g = 3$, which becomes more pronounced for $g = 5$ (the red solid and dashed lines, respectively). Using the current approach, we find a substantial reduction of the criti-
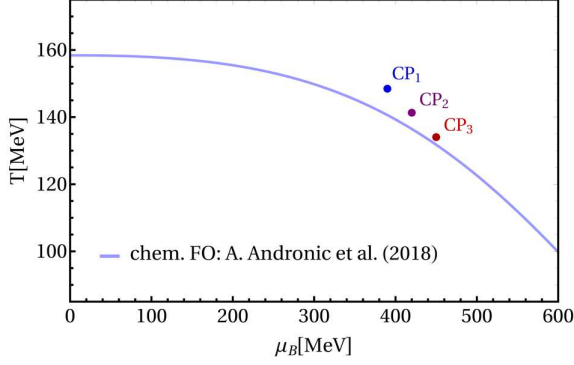
Fig. 2. (Color online) QCD critical point locations from Table plotted with the chemical freeze-out curve [15] used in this work
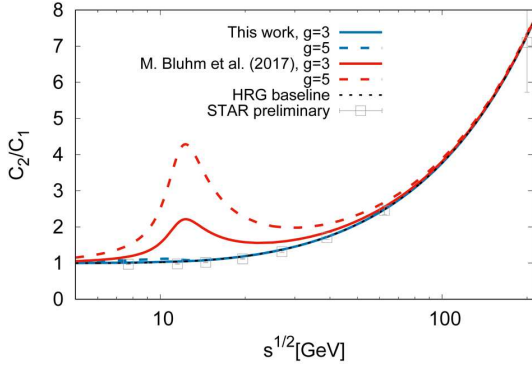

Fig. 3. (Color online) Second to first net-proton number cumulant ratio for $g = 3$ and 5 calculated following Ref. [10] (red solid and dashed lines, respectively) compared to the refined model results [11] (blue solid and dashed lines, respectively). The preliminary STAR data on the net-proton number fluctuations [5] (squares with the error bars containing both statistical and systematic errors) and HRG baseline result (black dotted line) are also shown for comparison

Locations of the QCD critical point in the (μ_B, T)-plane considered in this work. These locations in the QCD phase diagram are shown in Fig. 2

CP_i	μ_{cp} [MeV]	T_{cp} [MeV]
1	390	149
2	420	141
3	450	134

cality in the C_2/C_1 ratio even for larger values of g (see the blue curves in Fig. 3). The refined model results for the C_2/C_1 ratio agree with the experimental data from the STAR Collaboration [5]. On the other hand, the original model would require an exception-
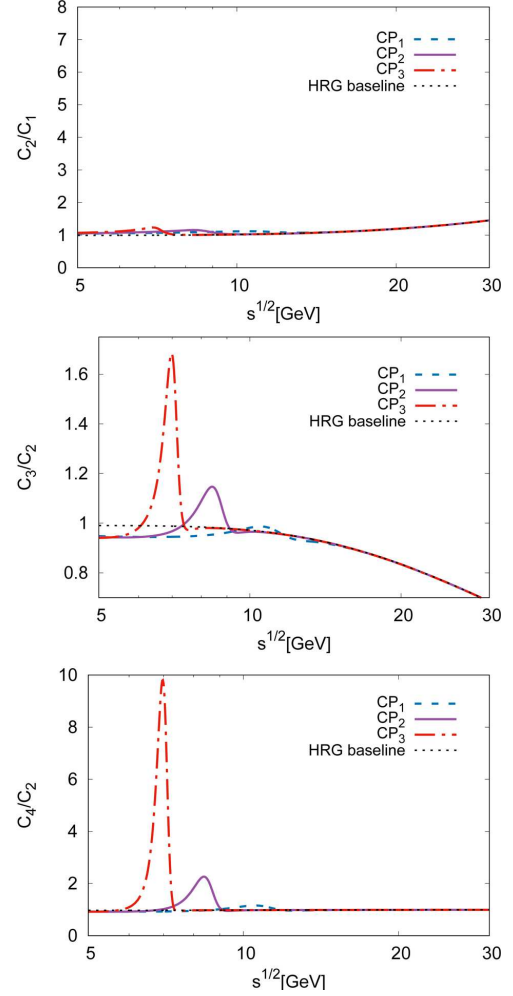

Fig. 4. (Color online) Ratios of net-proton number cumulants calculated in the refined model [11] for the fixed coupling $g = 5$ and for different locations of the QCD critical point (listed in Table)

ally small coupling strength in order to capture the experimentally observed behavior.

The net-proton cumulant ratios obtained in the refined model for different locations of the critical point (as listed in Table) and with a fixed value of the coupling, $g = 5$, are shown in Fig. 4. We find that a non-monotonic behavior of the cumulant ratios becomes more pronounced, when the critical point is closer to the freeze-out line. Moreover, the deviation from the non-critical HRG baseline becomes larger for higher-order cumulant ratios.

Finally, Fig. 5 shows the coupling strength dependence of the net-proton number cumulant ratios ob-
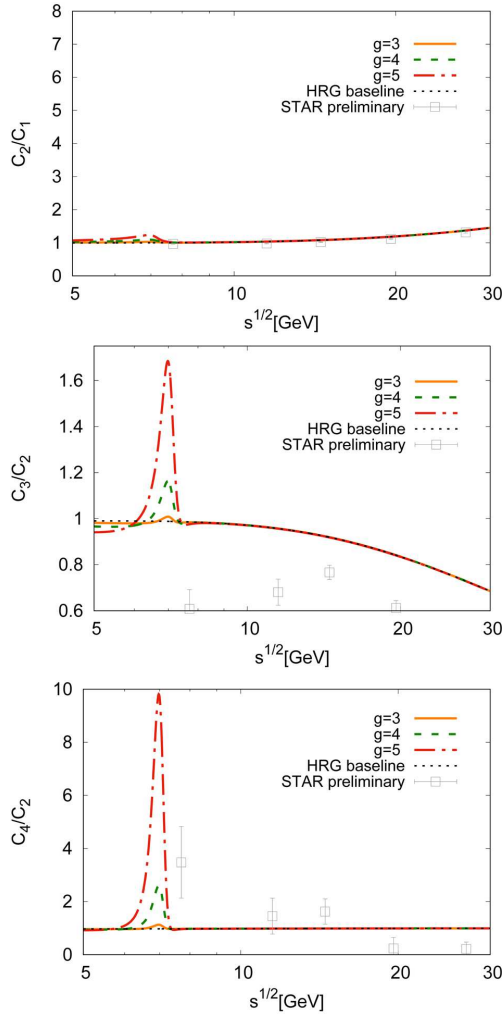
Fig. 5. (Color online) Ratios of net-proton number cumulants calculated in the refined model [11] with CP_3 and for the coupling strengths, $g = 3$, 4 and 5 (orange solid, green long-dashed, and red dash-dotted lines, respectively). The preliminary STAR data on the net-proton number fluctuations [5] (squares with the error bars containing both statistical and systematic errors) and HRG baseline results (black dotted lines) are also shown for comparison

tained for CP_3. We find a strong g dependence of all ratios. This is expected, since, in our refined model, the n-th cumulant scales as g^{2n}, according to Eqs. (7) and (11)–(13). When our model results are compared to the STAR data [5], we find a qualitative agreement with the C_2/C_1 and C_4/C_2 ratios. On the other hand, the C_3/C_2 ratio does not follow the systematics seen in the data, i.e., our model results overshoot the HRG baseline, while the data stay below.

Our results suggest that the appropriate choice of model parameters, as well as the location of the QCD critical point, allows us to describe some of the experimentally observed cumulant ratios. Especially, the smooth dependence of C_2/C_1 and the strong increase of C_4/C_2 at low beam energies, $\sqrt{s} < 20$ GeV, seen by the STAR Collaboration, suggest that the QCD critical point may be located close to the freeze-out curve. However, in this case, the C_3/C_2 ratio should increase beyond the non-critical baseline, which is not seen in the experimental data. Therefore, it seems unlikely that the QCD critical point is close to the freeze-out curve. This conclusion requires, however, additional theoretical and experimental justifications due to uncertainties in the model parameters as well as in the experimental data.

4. Conclusions

We have presented the ratios of net-proton number cumulants obtained within an effective model in which the coupling between (anti)protons and critical mode fluctuations is introduced by connecting the particle masses to the order parameter. We have modified the existing approach [10] to account for the correct scaling properties of the baryon number susceptibility, as dictated by the universality hypothesis.

Model results were compared with the recent experimental data on net-proton number fluctuations from the STAR Collaboration. We find a substantial reduction of the signal coming from the presence of the QCD critical point in the C_2/C_1 ratio which stays in agreement with the experimental data. Moreover, we find that the model discussed in the present work allows us to describe some of the experimentally observed features in the net-proton number cumulant ratios. Particularly, the smooth dependence of C_2/C_1 and an increase in C_4/C_2 at lower beam energies ($\sqrt{s} < 20$ GeV) suggest that the critical point may be located close to the freeze-out curve. However, the experimentally observed C_3/C_2 ratio does not follow the behavior expected from such a scenario.

Therefore, it seems unlikely that the QCD critical point is located close to the phenomenological freeze-out curve. However, because of uncertainties on both theoretical and experimental sides, this statement requires a further investigation.

1. M.A. Stephanov, K. Rajagopal, E.V. Shuryak. Signatures of the tricritical point in QCD. *Phys. Rev. Lett.* **81**, 4816 (1998).

2. M.A. Stephanov, K. Rajagopal, E.V. Shuryak. Event-by-event fluctuations in heavy ion collisions and the QCD critical point. *Phys. Rev. D* **60**, 114028 (1999).

3. X. Luo, [STAR Collaboration]. Energy dependence of moments of net-proton and net-charge multiplicity distributions at STAR. *PoS CPOD* **2014**, 019 (2015).

4. X. Luo. Exploring the QCD phase structure with beam energy scan in heavy-ion collisions. *Nucl. Phys. A* **956**, 75 (2016).

5. J. Thäder [STAR Collaboration]. Higher moments of net-particle multiplicity distributions. *Nucl. Phys. A* **956**, 320 (2016).

6. G.A. Almasi, B. Friman, K. Redlich. Baryon number fluctuations in chiral effective models and their phenomenological implications. *Phys. Rev. D* **96**, 014027 (2017).

7. F. Karsch. Lattice QCD results on cumulant ratios at freeze-out. *J. Phys. Conf. Ser.* **779**, 012015 (2017).

8. A. Bzdak, V. Koch. Net-baryon multiplicity distribution consistent with lattice QCD. *Phys. Rev. C* **99**, 024913 (2019).

9. V. Koch, A. Bzdak. Fluctuations and the QCD phase diagram. *Acta Phys. Polon. B* **47**, 1867 (2016).

10. M. Bluhm, M. Nahrgang, S.A. Bass, T. Schäfer. Impact of resonance decays on critical point signals in net-proton fluctuations. *Eur. Phys. J. C* **77**, 210 (2017).

11. M. Szymański, M. Bluhm, K. Redlich, C. Sasaki. Net-proton number fluctuations in the presence of the QCD critical point. *arXiv*:1905.00667 [nucl-th].

12. C. Sasaki, B. Friman, K. Redlich. Quark number fluctuations in a chiral model at finite baryon chemical potential. *Phys. Rev. D* **75**, 054026 (2007).

13. C. Sasaki, B. Friman, K. Redlich. Chiral phase transition in the presence of spinodal decomposition. *Phys. Rev. D* **77**, 034024 (2008).

14. J. Zinn-Justin. *Quantum Field Theory and Critical Phenomena* (Clarendon Press, 2002).

15. A. Andronic, P. Braun-Munzinger, K. Redlich, J. Stachel. Decoding the phase structure of QCD via particle production at high energy. *Nature* **561**, 321 (2018).

16. F. Wilczek. Application of the renormalization group to a second-order QCD phase transition. *Int. J. Mod. Phys. A* **07**, 3911 (1992).

17. A.M. Halasz, A.D. Jackson, R.E. Shrock, M.A. Stephanov, J.J.M. Verbaarschot. Phase diagram of QCD. *Phys. Rev. D* **58**, 096007 (1998).

18. H.-T. Ding, F. Karsch, S. Mukherjee. Thermodynamics of strong-interaction matter from Lattice QCD. *Int. J. Mod. Phys. E* **24**, 1530007 (2015).

19. Y. Hatta, T. Ikeda. Universality, the QCD critical/tricritical point and the quark number susceptibility. *Phys. Rev. D* **67**, 014028 (2003).

20. S. Mukherjee, R. Venugopalan, Y. Yin. Real time evolution of non-Gaussian cumulants in the QCD critical regime. *Phys. Rev. C* **92**, 034912 (2015).

21. C. Nonaka, M. Asakawa. Hydrodynamical evolution near the QCD critical end point. *Phys. Rev. C* **71**, 044904 (2005).

22. R. Guida, J. Zinn-Justin. 3-D Ising model: The scaling equation of state. *Nucl. Phys. B* **489**, 626 (1997).

23. B. Abelev *et al.*, [ALICE Collaboration]. Centrality dependence of π, K, p production in Pb–Pb collisions at $\sqrt{s_{NN}} = 2.76$ TeV. *Phys. Rev. C* **88**, 044910 (2013).

24. B.B. Abelev *et al.*, [ALICE Collaboration]. K_S^0 and Λ production in Pb–Pb collisions at $\sqrt{s_{NN}} = 2.76$ TeV. *Phys. Rev. Lett.* **111**, 222301 (2013).

25. B.B. Abelev *et al.*, [ALICE Collaboration]. Multi-strange baryon production at mid-rapidity in Pb–Pb collisions at $\sqrt{s_{NN}} = 2.76$ TeV. *Phys. Lett. B* **728**, 216 (2014), Erratum: [*Phys. Lett. B* **734**, 409 (2014)].

26. B.B. Abelev *et al.*, [ALICE Collaboration]. $K^*(892)^0$ and ffl(1020) production in Pb–Pb collisions at $\sqrt{sNN} = 2.76$ TeV. *Phys. Rev. C* **91**, 024609 (2015).

27. J. Adam *et al.*, [ALICE Collaboration]. $^3_\Lambda$H and $^3_\Lambda\overline{\text{H}}$ production in Pb–Pb collisions at $\sqrt{s_{\text{NN}}} = 2.76$ TeV. *Phys. Lett. B* **754**, 360 (2016).

28. J. Adam *et al.*, [ALICE Collaboration]. Production of light nuclei and anti-nuclei in pp and Pb–Pb collisions at energies available at the CERN large hadron collider. *Phys. Rev. C* **93**, 024917 (2016).

М. Шиманскі, М. Блум, К. Редліх, К. Сасакі

ПОШУКИ КРИТИЧНОЇ ТОЧКИ
КХД З ФЛУКТУАЦІЄЮ ЧИСЛА ПРОТОНІВ

Р е з ю м е

Флуктуації повного числа протонів можна вимірювати експериментально, отримуючи таким чином важливу інформацію про речовину, що народжується під час зіткнень релятивістських іонів. Зокрема вона може містити інформацію про критичну точку КХД. В даній роботі ми обговорюємо залежність відношень перших чотирьох кумулянтів числа протонів від енергії струменя частинок. Ці величини розраховані за допомогою феноменологічної моделі, в якій флуктуації з критичною модою пов'язані з протонами та антипротонами. Наша модель якісно відтворює як монотонну поведінку відношення найнижчих порядків, так і немонотонну поведінку відношень високих порядків, як це спостерігається в результатах колаборації STAR. Ми обговорюємо також залежність наших результатів від сили зв'язку і місцезнаходження критичної точки.